An application-oriented model for lock filling processes
by

Fabian Belzner[1], Franz Simons[1] and Carsten Thorenz[1]

1. INTRODUCTION

The German federal inland waterway network is the biggest waterway network in Western Europe with a length of 7,300 km. In 2016 about 221 million tons of cargo were transported on these waterways which equals 8 % of the whole transportation volume in Germany. Part of the waterway network are about 400 lock chambers which are key elements of the waterway infrastructure as they enable ships to overcome water level differences: These are located at impounded rivers, between sections of canals or at connection points. The safe and efficient operation of these locks is essential for the transport of goods on the waterways. One of the main tasks of the German Federal Waterway Engineering and Research Institute (German abbreviation: BAW) is to support the government in the design process of these locks in case of new construction or reconstruction. Ideally the costs for construction and operation of the locks can be minimized while still guaranteeing a short cycle time and a safe passage.

During the early planning period of a lock the hydraulic system has to be designed regarding several demands concerning structure, operation and safety. From a hydraulic point of view, a filling system has to be found that triggers minimal forces acting on the vessel and guarantees a short filling time. Every change on the filling system or the valve opening velocity can have a high influence on the forces acting on the ship and can result in breaking hawsers. An overview of the hydraulic and constructional needs of ship locks is given by Partenscky (1986) or in PIANC (2015).

Today, the determination of the forces acting on a vessel can be carried out by on-site measurements, physical or numerical models. On-site measurements are very complicated because a lock prototype and a real ship are needed. Measurement techniques must resist high forces, high pressures, flow velocities and in some cases very low temperatures and the measuring procedures must be safe for the ship and for the staff. The measuring period can be limited by factors like the amount of traffic or the weather conditions. Often only a few experiments are possible and the measurement techniques have to be planned carefully because there is no chance to change methodology during the experiments. Bousmar et al. (2017) describe these on-site measurements as essential for the diagnostic of existing locks but also mention the struggles of measuring under difficult circumstances.

During the design process of a new lock on-site measurements are impossible because often no prototype exists. The classical way to investigate and optimize planned locks is to conduct physical experiments at a scale model. Such experiments are e. g. described by Thorenz and Anke (2013) or Van der Ven et al. (2015). Scale models have the advantage that they can be constructed in a dry and heated laboratory and a large number of experiments can be conducted within a short time. However, the construction time of these models is at least several months, for complicated locks it can be even more than one year. The results can be influenced by scale effects or unwanted interaction between the model physics and the measurement technique and it is not possible to reproduce all relevant effects in a scale model. For example the strain behavior of the mooring lines is typically not reproduced in physical models, because the handling of the lines in reality is often unknown and difficult to predict. Nevertheless, physical scale modeling of locks is the most common method to determine forces acting on a vessel due to the high level of reliability and the large amount of experience available.

In line with the increasing computational power in the last years, a large progress in the development of multidimensional numerical methods happened (Thorenz 2009). Today it is possible to perform high resolution three dimensional simulations of transient hydromechanical phenomena like the filling of a lock. A number of methods to simulate the swimming vessel exist. However, these methods require high skill

---

[1] Federal Waterways Engineering and Research Institute, Germany, fabian.belzner@baw.de

levels and substantial computer power. The simulation time for a lock filling process with swimming vessel, moving valves etc. uses several days of computing time even on a cluster computer system and is therefore not yet suitable for the everyday-simulation of a large number of cases. The numerical elevation of the filling and emptying system of the new Panama Canal locks is given by Thorenz (2010), an overview on the numerical methods to simulate the lock filling process with OpenFOAM® is given by Thorenz et al. (2017),

For the early planning stage, but also for the assessment of small constructional changes in the final planning, both methods are not suitable. Carrying out physical or numerical model tests, takes often too much time. Therefore, simplified models are desirable, which consider the main hydraulic phenomena and allow a rough estimation and short-time prediction of the expected forces on the ship together with the filling times. For the most basic phenomena analytic equations are available. For a better approximation, more complex tools are necessary. An example is LOCKFILL which allows analyzing the filling and emptying of a lock chamber through the lock head (De Loor 2016). Lockfill is based on the super-positioning of the solutions for different equations which describe the flow field in the lock chamber which were derived from analytic considerations.

Experience has shown that the consideration of the wave propagation in the lock chamber is essential for the ship forces. Here, a tool is presented which is based on the 1D Saint-Venant equations and allows the simulation of a lock filling process to determine the forces acting on the vessel due to different hydraulic conditions. In this paper, we first describe the most important aspects of the hydrodynamics of the lock filling process. Following this, the numerical scheme of the new 1D lock model is described. Afterwards, we show results from a calibration using data from physical model tests, and we point out limitations of the model. The paper will end with a summary and conclusions on the presented topic. All symbols used in this paper are listed and explained in Section 7.

2. HYDRODYNAMICS OF THE LOCK FILLING PROCESS

During the filling process of a lock chamber with a through-the-gate system different phenomena can be observed which can interact with each other. The main phenomena causing longitudinal forces acting on a vessel are:

- - An initial surge wave triggered by the valve opening,
- - the propagation of a filling jet,
- - a water level slope due to the zero velocity boundary at the downstream end of the chamber,
- - dynamic effects like wave propagation in the chamber and
- - energy losses due to wall friction or contraction-expansion losses.

All the impacts of these phenomena have to be regarded to estimate the forces acting on the vessel during the lock filling process. The longitudinal forces acting on the vessel result from two predominant mechanisms: one is the downhill force resulting from a water surface slope; the other one is the force resulting from a filling jet hitting the vessel. The latter should be avoided in general. A further description can be found e.g. in Vrijburcht (1991).

The inflow in the lock chamber Q [m³/s] at any time can be expressed as a function of the pressure difference Δh [m], the valve opening area A_{valve} [m²] and a dimensionless discharge coefficient μ [-] which takes into account the geometry of the control section. The discharge coefficient can be estimated from literature, physical or numerical models. For the sluice gate type of valve it is usually between 0.6 and 1.0. Note: Δh is the maximum available pressure difference, i. e. for submerged filling systems it is the difference between the water levels in the upstream outer harbor and the lock chamber and for free flow it is the maximum pressure height over the control section. The inflow into the lock chamber can be calculated from:

$$Q = \mu \cdot A_{\text{valve}} \cdot \sqrt{2g \cdot \Delta h} \tag{1}$$

For a known gross area of the lock chamber A_{chamber} [m²], the water level development can be computed from:

$$\frac{dh}{dt} = \frac{Q}{A_{\text{chamber}}} \tag{2}$$

At the beginning of the lock filling process a first surge wave, triggered by the inflow gradient, results in a slope in downward direction. The slope resulting from this first flush I_{flush} [-] is proportional to the gradient of the inflow:

$$I_{\text{flush}} = -\frac{\mathrm{d}Q}{\mathrm{d}t \cdot (W_{\text{chamber}} \cdot h - A_{\text{vessel}})} \tag{3}$$

where W_{chamber} [m] is the chamber width and A_{vessel} [m²] is the cross sectional area of the vessel. According to equation (1) the inflow in the lock chamber scales almost linear with the valve opening velocity. Therefore, the water level slope due to the first flush scales also linearly with the valve opening velocity. For locks with large lift heights and potent energy dissipation at the lock head, the force resulting from this surge wave may become dominant. This initial force can be minimized by reducing the initial valve opening velocity for a certain time at the beginning of the filling process. As the discharge in this early period is small anyway, the reduction of the initial valve opening velocity will hardly increase the filling time. Figure 1 (a) shows this slope and the resulting force in downstream direction. After this first flush a velocity distribution from the upstream to the downstream edge of the lock chamber is developing.
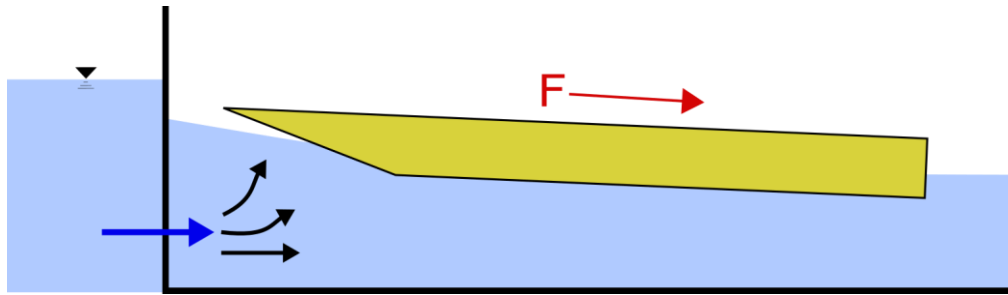
(a) Water level slope in downstream direction due to first flush
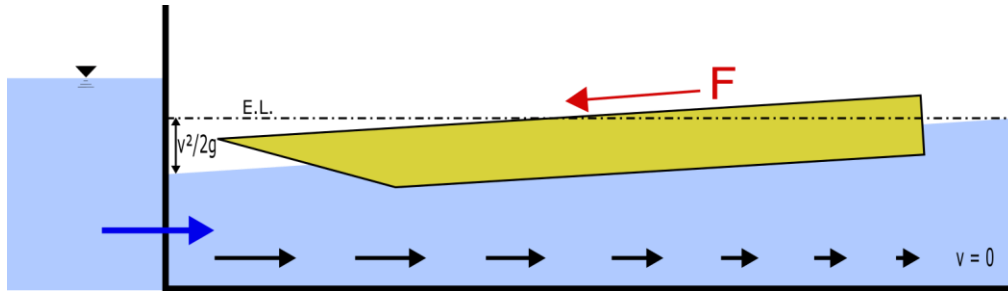
(b) Water level slope in upstream direction due to decreasing velocity

Figure 1: Temporal progression of ship forces during lock filling process

With an "ideal" energy dissipation at the lock head, the mean velocity u_{mean} [m/s] behind the upstream inlet corresponds to the inflow divided by the available cross sectional area of the lock chamber:

$$u_{\text{mean}} = \frac{Q}{W_{\text{chamber}} \cdot h - A_{\text{vessel}}} \tag{4}$$

The downstream gate of the lock chamber is closed during the filling process. Thus, the velocity at the end of the chamber is zero. Assuming a constant total head in the lock chamber and a linear decreasing velocity head from the upstream to the downstream edge like it is shown in Figure 1 (b), a stationary sloped water surface I_{stat} [-] in upstream direction is developing to compensate the decreasing velocity head. Consequently, this slope depends on the inlet velocity u_{mean} and the length of the lock chamber L_{chamber} [m] and can be calculated by (5).

$$I_{\text{stat}} = \frac{u_{\text{mean}}^2}{2 \cdot g \cdot L_{\text{chamber}}} \tag{5}$$

Considering the longitudinal forces as downhill forces and neglecting the jet near the vessel and other dynamic phenomena, the forces acting on the ship can be roughly estimated from the water level slope around the vessel by summing up the slopes and multiplying by the mass of the vessel m_{vessel} [kg]:

$$F = (I_{\text{flush}}^n + I_{\text{stat}}^n) \cdot m_{\text{vessel}} \tag{6}$$

The surge waves are propagating in the chamber and are reflected at the upstream and downstream ends. As a result sloshing occurs. The cycle time T [s] can be calculated by the shallow water wave celerity equation and the geometry of the chamber and the vessel:

$$T = 2 \cdot \left(\frac{L_{\text{chamber}} - L_{\text{vessel}}}{\sqrt{g \cdot h}} + \frac{L_{\text{vessel}}}{\sqrt{g \cdot \left(h - \frac{A_{\text{vessel}}}{W_{\text{chamber}}} \right)}} \right) \tag{7}$$

A first approximation of the forces acting on the vessel during the lock filling process can be done without great effort using equation (6). Substantial dynamic effects like wave propagation, the influence of the filling jet, friction losses or the development of the forces over the time are neglected in this simplified approach. Nevertheless this approach allows a rough approximation of the forces acting on a vessel using a pocket calculator within a few minutes. But it must be pointed out that dynamic effects can have a huge and dominant influence on the results and these are neglected here. Thus, a more sophisticated approach should be used.

3. 1D LOCK MODEL

3.1. Introduction

Due to the deficiencies of the simplified analytic approaches it was decided, to implement a 1D model for the lock filling process. It was assumed, that this is more straight-forward than the adaptation of the analytical approximations to more complex situations and the super-positioning of effects. Furthermore, the 1D approach offers the possibility for future enhancements, e.g. the coupling to 1D pipe network models in order to simulate more complex filling systems.

3.2. Basic equations

The flow in a lock chamber in case of filling from the head has a strong domination in longitudinal chamber direction. The water surface is assumed to be horizontal, a hydrostatic pressure distribution is predominant and the energy slope is small. Neglecting phenomena which might cause lateral water level slopes and forces, the flow in the lock chamber can be described by the one dimensional (1D) Saint-Venant equations which allow the calculation of the water depth and a mean flow velocity in discrete cross sections in the chamber. The 1D Saint-Venant equations are a set of two partial differential equations describing the conservation of mass and momentum in channel flow. The derivation and several numerical approaches for a solution of these equations are described by Cunge et al. (1980). Using the two main variables Q [m³/s] and A [m²], the 1D Saint-Venant equations are given in a conservative formulation as (Jirka, Lang 2009):

$$\frac{\partial A}{\partial t} + \frac{\partial Q}{\partial x} = q \tag{8}$$

$$\frac{\partial Q}{\partial t} + \beta \cdot \frac{\partial}{\partial x} \cdot \left(\frac{Q^2}{A} \right) + g \cdot A \cdot \frac{\partial h}{\partial x} = g \cdot A \cdot (I_{\text{o}} - I_{\text{e}} - I_{\text{R}}) \tag{9}$$

I_{o}, I_{e} and I_{R} in equation (9) are the slopes due to a sloped bed, local contraction-expansion losses and friction. The longitudinal forces acting on the ship can be derived from the water level gradient.

3.3. Consideration of the filling jet

One requirement for using the 1D Saint-Venant equations is the assumption of a uniform flow distribution within every cross section. In reality a filling jet can develop from the upstream gate leading to a strongly non-uniform velocity distribution because of the high velocity inside of the jet and small velocities in the surrounding (cf. Figure 9). Due to the proportionality of the local momentum flux to the square of the local velocity, the mean flow velocity cannot be used anymore to calculate the convective acceleration in equation (9). To correct this, the Boussinesq coefficient β [-] is commonly used which regards the ratio of the mean flow velocity $\bar{u}$ [m/s] and the sum of local flow velocities in the jet. Here we are regarding a discretized version, where A [m²] is the overall cross sectional area which can be divided in K areas A_k [m²] with the velocities u_k [m/s]:

$$\beta = \frac{\sum_0^K u_k^2 \cdot A_k}{\bar{u}^2 \cdot A} \tag{10}$$

Assuming only two cross sectional areas A (the whole cross sectional area) and A_{jet} [m²] (the subarea of A with the jet in it), equation (10) can be simplified to:

$$\beta = \frac{A}{A_{\text{jet}}} \tag{11}$$

Due to the balance of the convective acceleration and the gradient of h in equation (9) for constant discharges, a lowering of the water level is the consequence of high β values resulting from a distinct jet. This must be reproduced in order to model the influence of a filling jet on a vessel. The effect can also be observed in physical experiments for locks with little energy dissipation at the upstream head.

3.4. Consideration of the vessel

The modeling of a swimming vessel with a 1D hydrodynamic approach is difficult and leads to a complicated solution. Thus, here a simplified approach was chosen. The ship is approximated by reducing the cross sectional area in the region of the vessel by the cross sectional area of the ship A_{vessel} [m²]. This is done initially for every cross section of the model by computing the wetted cross sectional area of the lock from:

$$A = h \cdot W_{\text{chamber}} - A_{\text{vessel}} \tag{12}$$

During the simulation gradients of the water surface are computed from the wetted cross sections. As the cross sectional area of the lock chamber decreases at the bow and increases at the stern without causing a gradient in the water level, the computation of the spatial gradient of h according to equation (9) must be adjusted by the vessel area:

$$\frac{\partial h}{\partial x} = \frac{\partial (A + A_{\text{vessel}})}{\partial x \cdot W_{\text{chamber}}} \tag{13}$$

3.5. Discretization

Due to the absence of an analytical solution for the 1D Saint-Venant equations a finite difference approach for the discretisation in space and time was chosen. Hereinafter the index i is denoting the current point in space, $i - 1$ and $i + 1$ are the grid points in front of and behind the point i (Figure 2). The index n denotes the current time step, $n + 1$ the next time step and $n - 1$ the previous time step. Δt is the size of one time step and Δx is the distance between two cross sections. For discretisation in space a staggered grid was chosen. The cross sectional area $A_{i+1/2}$ is calculated between the two cross sections i and $i + 1$, where the discharges Q_i and Q_{i+1} are calculated. This strategy has stability advantages and is comparable to the finite volume approach, where the flux is calculated at the faces of each cell.
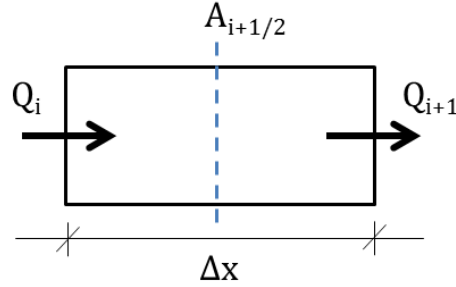
Figure 2: Points of calculation of A and Q

For the discretization in time the Crank-Nicolson method was used in order to obtain second order accuracy in time. The gradients between two cross sections can be calculated at half a time step or can be shifted by the Crank-Nicolson factor θ [-] like it is shown in equation (14) for the cross sectional area and in equation (15) for the discharge:

$$A^{n+\theta} = (1-\theta) \cdot A^{n+1} - \theta \cdot A^n \tag{14}$$

$$Q^{n+\theta} = (1-\theta) \cdot Q^{n+1} - \theta \cdot Q^n \tag{15}$$

For $\theta = 0$ the gradients are taken explicitly from the known time step, for $\theta = 1$ the gradients are taken implicitely from the future time step and for $\theta = 0.5$ a second order accuracy in time is obtained. A detailed description of the method can is given by Crank et al. (1947).

The derivations from the continuity equation (8) were discretisized in the following manner:

$$\frac{\partial A}{\partial t} = \frac{A_{i+1/2}^{n+1} - A_{i+1/2}^n}{\Delta t} \tag{16}$$

$$\frac{\partial Q}{\partial x} = \frac{Q_{i+1}^{n+\theta} - Q_i^{n+\theta}}{\Delta x} \tag{17}$$

Discretising equation (8) with equations (16) and (17) and solving it for the wanted variable $A_{i+1/2}^{n+1}$ for the future time step $n+1$ leads to (18):

$$A_{i+1/2}^{n+1} = A_{i+1/2}^n - \frac{\Delta t}{\Delta x} \cdot (Q_{i+1}^{n+\theta} - Q_i^{n+\theta}) + \Delta t \cdot q_i \tag{18}$$

The discretisation of the parts of the momentum equation (9) is more complicated due to the non-linear terms:

$$\frac{\partial Q}{\partial t} = \frac{Q_i^{n+1} - Q_i^n}{\Delta t} \tag{19}$$

$$\beta \cdot \frac{\partial}{\partial x} \cdot \left(\frac{Q^2}{A}\right) = \left(\beta_i \cdot \frac{Q_{i+1/2}^{n+\theta} \cdot Q_{i+1/2}^{n+\theta}}{A_{i+1/2}^{n+\theta}} - \beta_{i-1} \cdot \frac{Q_{i-1/2}^{n+\theta} \cdot Q_{i-1/2}^{n+\theta}}{A_{i-1/2}^{n+\theta}}\right) \cdot \frac{1}{\Delta x} \tag{20}$$

$$g \cdot A \cdot \frac{\partial h}{\partial x} = g \cdot \frac{1}{2} \cdot \left(A_{i+1/2}^{n+\theta} - A_{i-1/2}^{n+\theta}\right) \cdot \frac{(A + A_{\text{vessel}})_{i+1/2}^{n+1} - (A + A_{\text{vessel}})_{i-1/2}^{n+1}}{\Delta x \cdot W_{\text{chamber}}} \tag{21}$$

$$g \cdot A \cdot (I_{\text{o}} - I_{\text{e}} - I_{\text{R}}) = g \cdot \frac{1}{2} \cdot \left(A_{i+1/2}^{n+\theta} - A_{i-1/2}^{n+\theta}\right) \cdot (I_{\text{o}} - I_{\text{e}} - I_{\text{R}}) \tag{22}$$

Discretising equation (9) with equations (19), (20), (21) and (22) and solving it for the wanted variable Q_i^{n+1} for the future time step $n+1$ leads to equation (23):

$$Q_i^{n+1} = Q_i^n - \frac{\Delta t}{\Delta x} \cdot \beta_i \cdot \frac{Q_{i+1/2}^{n+\theta} \cdot Q_{i+1/2}^{n+\theta}}{A_{i+1/2}^{n+\theta}} + \frac{\Delta t}{\Delta x} \cdot \beta_{i-1} \cdot \frac{Q_{i-1/2}^{n+\theta} \cdot Q_{i-1/2}^{n+\theta}}{A_{i-1/2}^{n+\theta}} - \Delta t \cdot g \cdot \frac{1}{2} \cdot \left(A_{i+1/2}^{n+\theta} - A_{i-1/2}^{n+\theta} \right)$$
$$\cdot \frac{(A + A_{\text{vessel}})_{i+1/2}^{n+1} - (A + A_{\text{vessel}})_{i-1/2}^{n+1}}{\Delta x \cdot W_{\text{chamber}}} + \Delta t \cdot g \cdot \frac{1}{2} \cdot \left(A_{i+1/2}^{n+\theta} - A_{i-1/2}^{n+\theta} \right) \cdot (I_e + I_R) \tag{23}$$

3.6. Boundary conditions

As boundary conditions a zero flux condition is applied for the downstream end of the lock chamber. The solver core allows adding fluxes and also the specification of the momentum transported with the flux at any point of the lock chamber. The fluxes are added as sources to the continuity equation and the momentum equation. In the following, we are regarding the simplified case of a through-the-head system. In this case, the fluxes are added to the first node of the mesh. The inflow is calculated by equation (1) depending on the water level difference Δh between the lock chamber and the upstream harbor, the effective valve opening area A_{valve} and a discharge coefficient μ. The water level difference can be determined from the known upstream water level and the chamber water level of the previous time step. The valve opening area A_{valve} is a prescribed function of time and also known. The discharge coefficient μ describes the performance of the valve as a function of the valve opening. It can be determined a-priori with physical models or numerical simulations or, though with lower reliability, values from prior projects with similar geometry can be used. If prototype measurements or a physical model of a lock with the same valve geometry exist, the discharge coefficients can be determined by a comparison of the water levels over the time.

3.7. Solution procedure

The equations (18) and (23) allow the calculation of the cross sectional area A and the discharge Q for every cross section for the time step $n + 1$. But this requires the values of A and Q at the Crank-Nicolson time step $n + \theta$, which would lead to an implicit solution algorithm. To avoid the solution of a non-linear equation system, a predictor-corrector method was used. At the beginning of the first predictor-corrector loop the values for the future time step $n + 1/2$ are predicted by the explicit Adam-Bashforth multistep method like shown in equations (24) and (25):

$$Q^{n+\frac{1}{2}} = Q^n + \frac{Q^n - Q^{n-1}}{\Delta t} \cdot \frac{1}{2} \cdot \Delta t = 1.5 \cdot Q^n - 0.5 \cdot Q^{n-1} \tag{24}$$

$$A^{n+\frac{1}{2}} = A^n + \frac{A^n - A^{n-1}}{\Delta t} \cdot \frac{1}{2} \cdot \Delta t = 1.5 \cdot A^n - 0.5 \cdot A^{n-1} \tag{25}$$

Assuming a constant gradient, the Adam-Bashforth method predicts the value of a future time step from the known time step and the gradient between the current and the previous time steps (Zhao, Zhang 2011). As a result of the extrapolation to $n + 1/2$ a Crank Nicolson factor of $\theta = 0.5$ is used for the first prediction. With $Q^{n+1/2}$ from equation (24) the discretized continuity equation (18) is solved for the first time. The result A^{n+1} is weighted with the Crank Nicolson equation (14). The results $A^{n+\theta}$ from equation (14) and $Q^{n+1/2}$ from equation (24) are used to solve the momentum equation (23) for Q^{n+1} which is weighted with equation (15). After the first predictor loop is finished, $A^{n+\theta}$ and $Q^{n+\theta}$ exist and the equations (18) and (23) are solved again to correct A^{n+1} and Q^{n+1} in a first correction loop. From the results a better value for $A^{n+\theta}$ and $Q^{n+\theta}$ can be calculated by equations (14) and (15) leading to better results for A^{n+1} and Q^{n+1} in additional correction loops. Equations (18) and (23) are solved fully explicit for $\theta = 0$, implicitly for $\theta = 1$ and for $\theta = 0.5$ the scheme has second order accuracy in time. With this implicit scheme a solution can be obtained after some iterations without having to solve a linear equation system. A graphical representation of the algorithm can be seen in Figure 3.
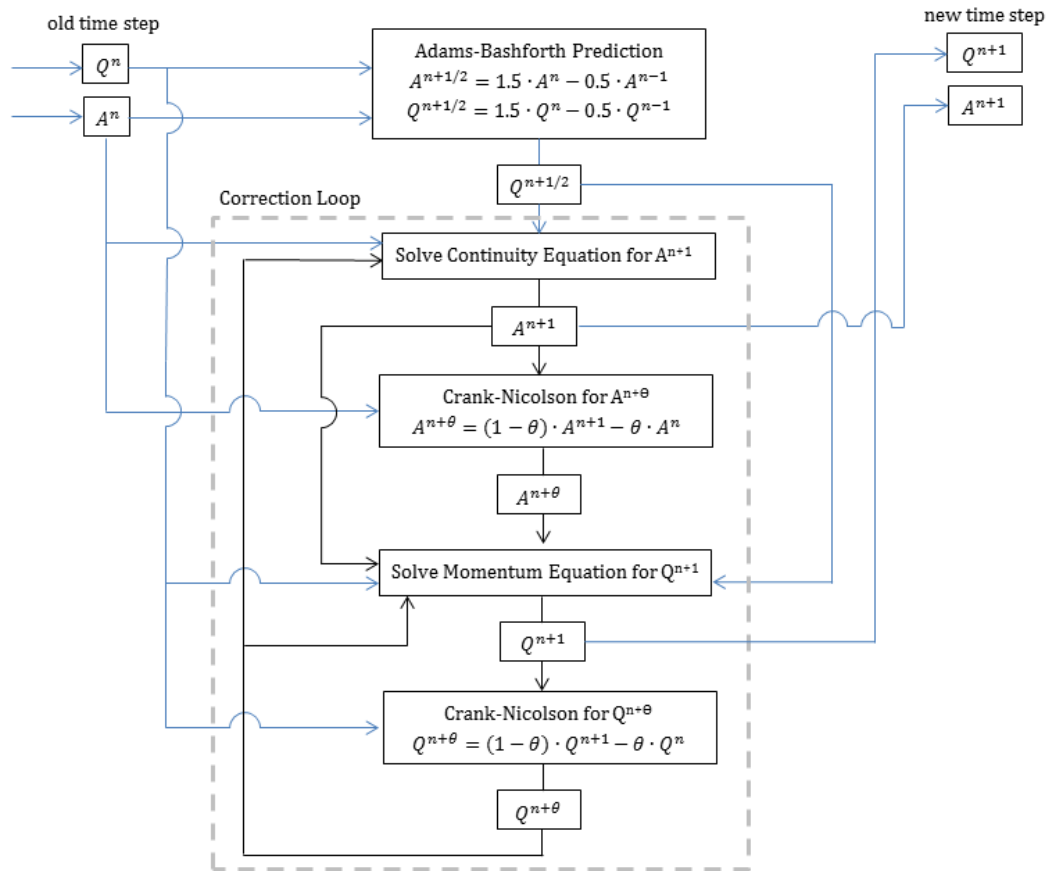
old time step

Q^n

A^n

Adams-Bashforth Prediction
$$A^{n+1/2} = 1.5 \cdot A^n - 0.5 \cdot A^{n-1}$$
$$Q^{n+1/2} = 1.5 \cdot Q^n - 0.5 \cdot Q^{n-1}$$

new time step

Q^{n+1}

A^{n+1}

$Q^{n+1/2}$

Correction Loop

Solve Continuity Equation for A^{n+1}

A^{n+1}

Crank-Nicolson for $A^{n+\theta}$
$$A^{n+\theta} = (1-\theta) \cdot A^{n+1} - \theta \cdot A^n$$

$A^{n+\theta}$

Solve Momentum Equation for Q^{n+1}

Q^{n+1}

Crank-Nicolson for $Q^{n+\theta}$
$$Q^{n+\theta} = (1-\theta) \cdot Q^{n+1} - \theta \cdot Q^n$$

$Q^{n+\theta}$

Figure 3: Predictor-Corrector solution scheme

3.8. Software implementation

Based on the presented numerical algorithms the tool LoMo (short form of "BAW Lock Model") was implemented, which simplifies the usage and provides a graphical representation of the results. LoMo is developed in the object-oriented programming language Java. Due to the platform independency of Java byte code, the releases can be executed on all major operating systems.

The computational core of LoMo is strictly separated from the graphical user interface using the model-view-controller design pattern (Gamma 2011). The graphical user interface (Figure 4) is based on the JavaFX library and can be easily internationalized using the Java ResourceBundle concept (Oracle 2018a). Currently, English and German internationalizations are available. Case setups can be stored to and read from XML files using the Java XML binding (JAXB) library (Oracle 2018b). The software design intends to simplify the extension by new chamber filling methods.

The BAW actively supports the Open Access policy of the German federal government. We signed the "Berlin Declaration on Open Access to Knowledge in the Sciences and Humanities" (Max-Planck-Gesellschaft 2003) in 2016 and declared an own open access guideline. In the spirit of this guideline the software is freely available and open source, licensed under the GNU General Public License 3 (Free Software Foundation 2007). Source code and releases can be found at GitHub (https://github.com/baw-de/lomo). You are welcome to test the software, to participate in the development and to give us feedback on GitHub. There is, however, no warranty for the accuracy and meaningfulness of the results.
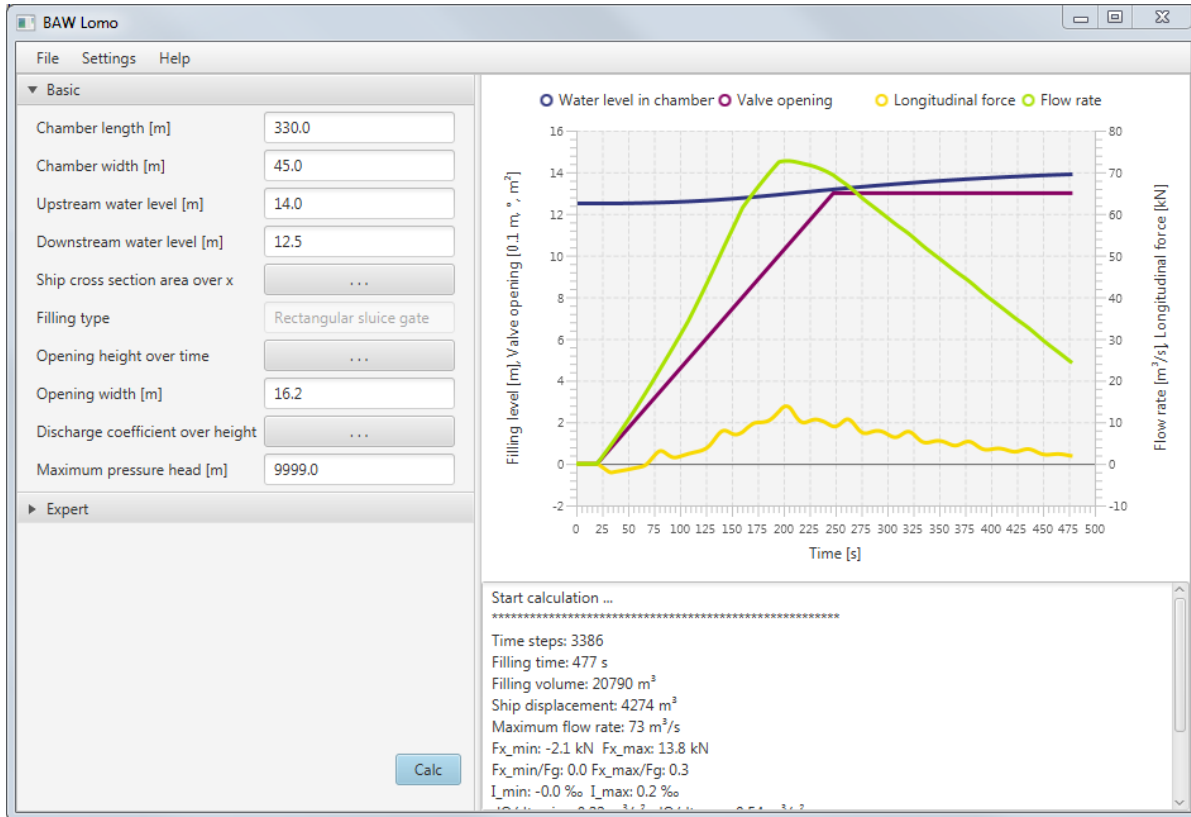
Figure 4: Graphical User Interface

3.9. Setup and Calibration parameters

The model is setup with the physical dimensions of the lock chamber and of the vessel in the lock chamber. Furthermore, the valve and filling system characteristics must be chosen and a valve opening curve must be defined. The calibration of the model can be carried out by comparing the results with laboratory results, results from three-dimensional numerical models or on-site measurements. There are two most important calibration parameter groups:

- The hydraulic performance of the filling system influencing the filling time and triggering waves. This is calibrated by the discharge coefficient as a function of the valve opening.
- The propagation of the jet which leads to a water level decrease and a slope in upstream direction.

Both parameters strongly influence the longitudinal forces acting on the vessel and have to be calibrated by known results.

4. COMPARISON WITH PHYSICAL MODEL RESULTS

4.1. Introduction

For calibration and validation purposes, several physical model results of the BAW were used. Here we present a model that was originally constructed for the validation of 3D numerical methods. Due to the objective of the physical model it was constructed as a very simple lock with one sluice gate valve and a continuous bottom between upstream outer harbor and the lock chamber. The vessel had the geometry of a push barge with a length of 3.01 m and a width of 0.46 m. The lock chamber had a hydraulic length of

6.32 m and a width of 0.48 m. The drop height was 0.08 m. Further dimensions are shown in Figure 6. The water level in the upstream outer harbor was kept constant by a labyrinth weir (Belzner et al. 2017). Several experiments with different valve opening velocities and ship positions in the chamber were performed to validate and calibrate the 1D model. The forces acting on the vessel during the lock filling process were determined by measuring the displacement of a spring bar. Additionally the water levels were determined by floating water level gauges. The inlet flow was determined from the temporal variation of the water level in the lock chamber. Figure 5 shows a detailed view of the upper part of the lock chamber with the gate (left), the vessel and the floating water level gauges. A further description of the evaluation of forces acting on a vessel with physical models is given by Thorenz, Anke (2013).
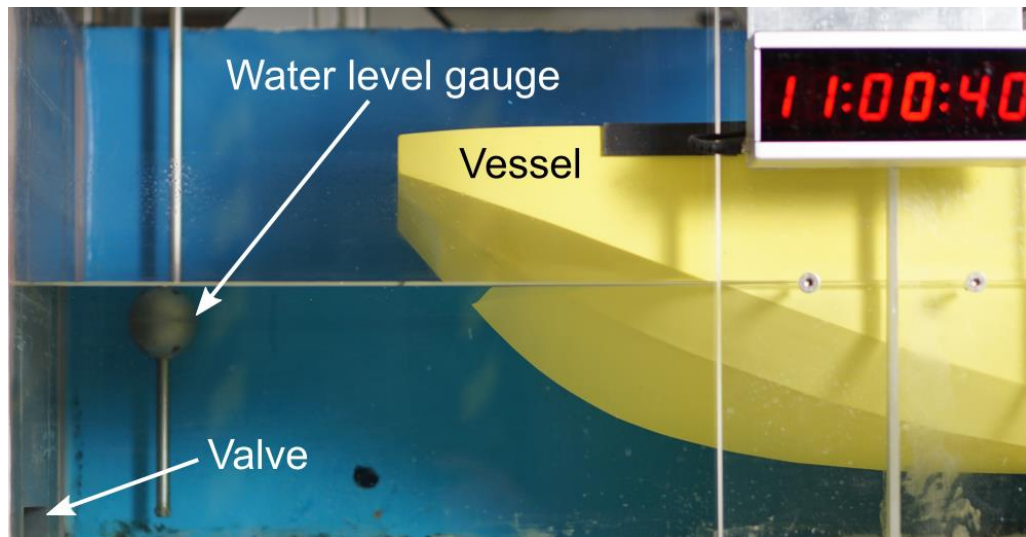

**Figure 5: Photo of the inlet section of the physical model**

4.2. Calibration of the hydraulic parameters of the filling system

After the known geometric properties were incorporated into the model, the unknown hydraulic parameters have to be calibrated. These are mainly the discharge coefficient as a function of the valve opening and the jet coefficients. Figure 7 shows the discharge coefficient depending on the valve opening for a typical sluice gate valve. The discharge coefficient was determined by a comparison of the inflow calculated from the results of a physical model with the inflow calculated by the 1D model with same geometrical boundary conditions and the same valve geometry and opening velocity.

Figure 8 shows a case which was used for the calibration of the discharge coefficient by comparison of the results determined with the physical model and calculated by the 1D model. The purple line shows the valve opening. The valve is opened in 390 s. The red and dark blue lines show the water levels measured in the laboratory model and calculated with the 1D model, respectively. For calibration the light blue and green lines which show the inflow in the laboratory and 1D models were regarded. The discharge coefficient depending on the valve opening position was adjusted until a good match between the light blue and the green lines was reached for the rising branch of the inflow.

It must be noted that discontinuities in the discharge coefficient or the valve opening velocity trigger waves running through the chamber and thus must be avoided. The forces acting on the vessel are downhill forces which react on waves. Thus, discontinuities in the discharge coefficient directly affect the longitudinal forces acting on the vessel.
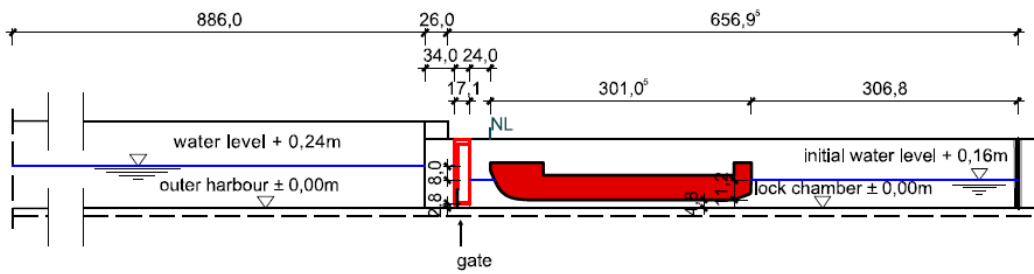
Plan view
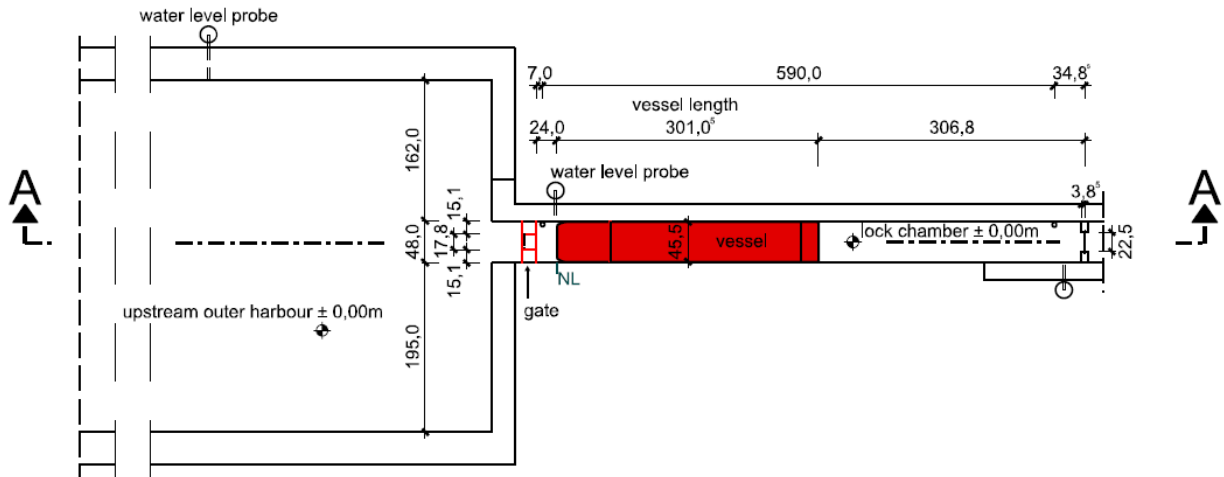
Slice A-A
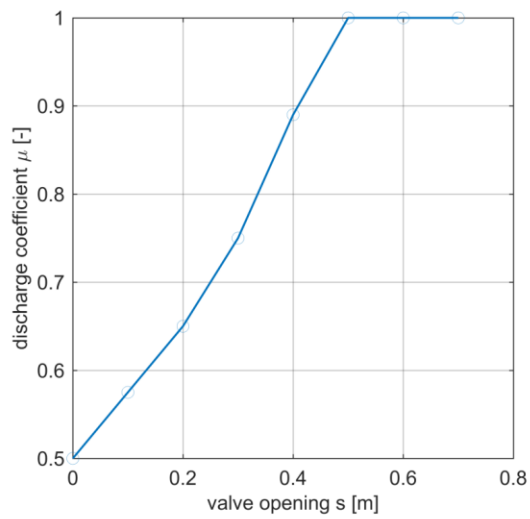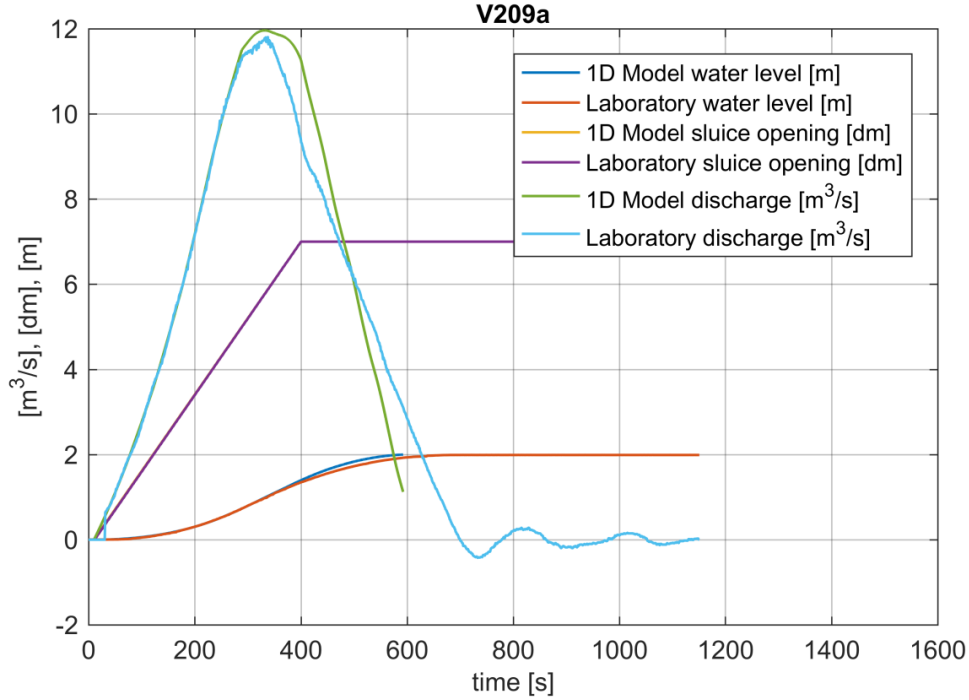

Figure 6: Construction plan of the physical model

Figure 7: Discharge coefficient depending on valve opening

V209a

**Figure 8: Calibration case for valve discharge coefficient
with 1.8 mm/s valve opening velocity**

4.3. Propagation of the jet

According to equation (11) the value β is reciprocal proportional to the jet area in every cross section which requires a description of the jet propagation in time and space. Figure 9 shows the upstream gate of a lock with a through-the-head filling system and a possible propagation of a filling jet inside the lock chamber. This jet results from a small valve opening area compared to the cross sectional area of the lock chamber. The cross sectional area of the jet is at least equal to the valve opening area, grows with increasing distance from the upstream head and cannot exceed the cross sectional area of the lock chamber. In-between these limits the shape of the jet has to be described by a function of time and space. The valve opening area and thus the initial jet cross section changes over time because the valve opening is a prescribed function of time. The jet cross section in the lock chamber is the sum of the initial jet cross section and the growing depending on the distance to the gate. This growth can be parameterized with a linear coefficient and an exponent.

The expansion rate of the jet is described with a linear coefficient c_2 and an exponent c_3 in equation (26) assuming that the initial jet cross section at the upstream head is a function of the current valve opening area A_{valve} [m²] and the coefficients c_0 and c_1.

$$A_{\text{jet}} = c_0 + c_1 \cdot A_{\text{valve}}(t) + c_2 \cdot x^{c_3} \tag{26}$$

For a linear spreading of the jet area the coefficient c_3 is equal to one, for a quadratic spreading c_3 is equal to two. For a flat, wide jet close to the ground a linear increase of the jet cross section over the length can be assumed. For a free circular jet a quadratic growth can be assumed. The description of the jet is complex and might change during the further development of the BAW lock model.
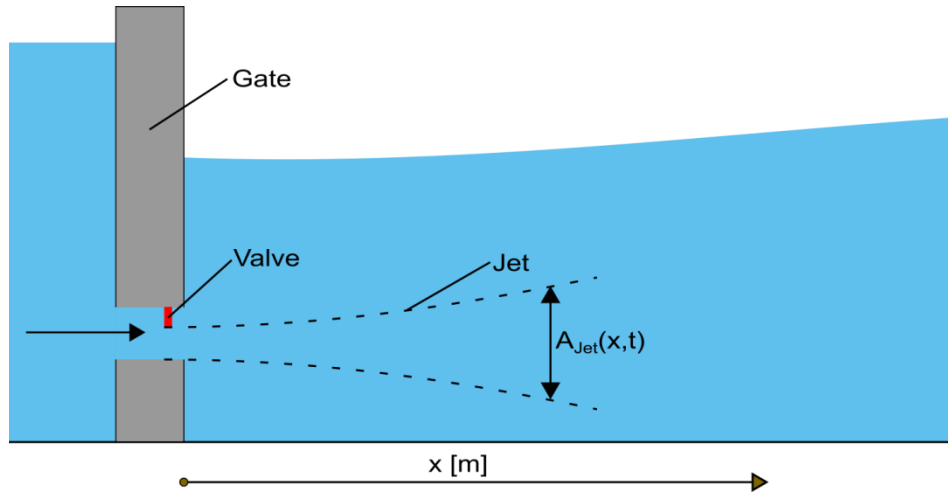
Figure 9: Propagation of the filling jet, definition sketch

Due to a strong dependency of the forces acting on the vessel from the ratio of jet cross section to chamber cross section a good parameterization of the jet propagation is significant for proper results. The parameterization can only be conducted by a comparison of the forces observed at the prototype or in physical experiments with the forces calculated by the 1D model. The thinner the jet, the more distinct is the water level slope to the upstream head and thus the forces acting in upstream direction. The initial jet cross section is described by the coefficients c_0 and c_1. For an initial jet cross section which equals the valve opening area c_0 can be set to $c_0 = 0$ and c_1 to $c_1 = 1$. The coefficients c_2 and c_3 must be parameterized to describe the jet propagation over the whole distance. Thus, at least two experiments must be carried out for calibration, one with the vessel close to the upstream head and one with the vessel more apart from the head. The forces calculated with the 1D model must fit both experiments as good as possible. Figure 10 shows a comparison of the calculated forces with the forces determined in physical experiments. The left subfigure shows the comparison with an experiment where the vessel position was close to the upstream head, the right subfigure shows the comparison with an experiment where the vessel position was in the middle of the lock chamber.
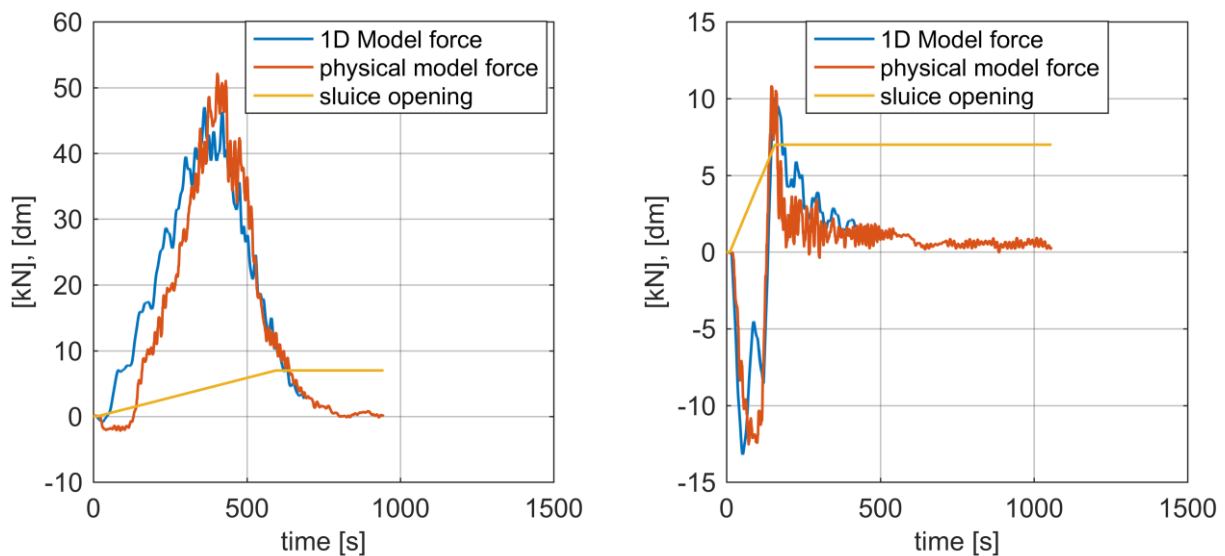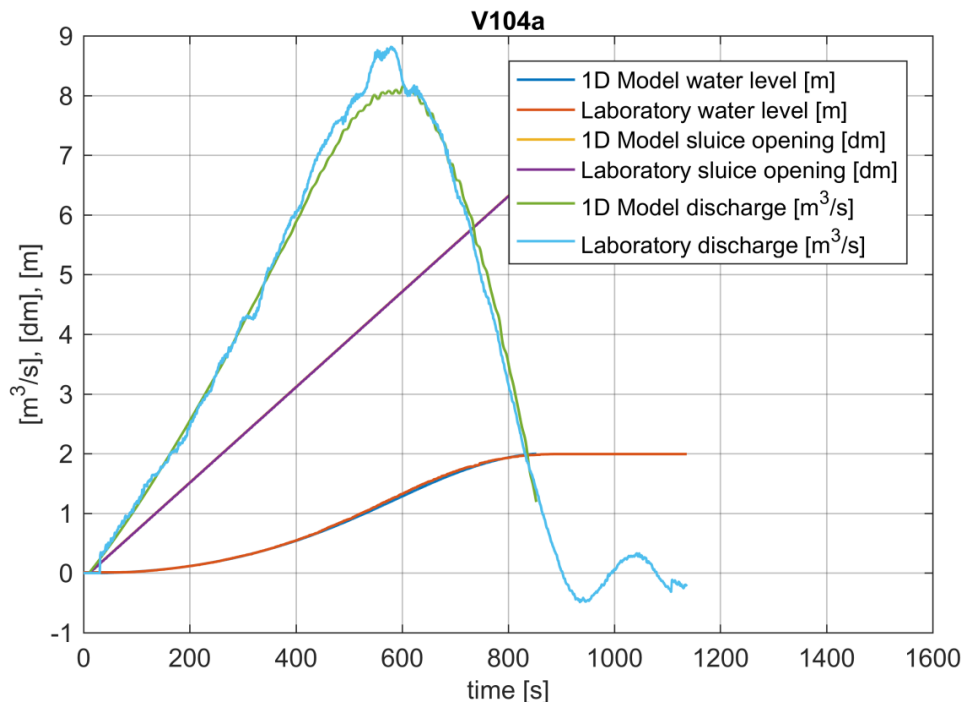

Figure 10: Calibration Case: Comparison of measured and simulated forces acting on a vessel for different vessel positions and valve opening velocities. left: vessel position near the upstream head, right: vessel in position in the middle of the lock chamber

4.4. Validation with physical model results

After the hydraulic parameters for the discharge and the jet propagation were calibrated, additional runs of the physical model were used for the validation of the model behavior. For the validation procedure the experiment was repeated with the previously determined values for the discharge coefficient but a smaller valve opening velocity. Here, the valve was opened in more than 800 s. The results are shown in Figure 11. Regarding the discharges, a very good agreement for both the rising side and the falling side of the discharge curve can be found.

For the further validation, the forces acting on the vessel were evaluated. The results of the validation experiments are shown in Figure 12. The calculated forces show a good agreement with the forces determined in the physical model. The left subfigure shows the comparison with an experiment where the vessel position was close to the upstream head, the right subfigure shows the comparison with an experiment where the vessel position was in the middle of the lock chamber.

In Figure 12 (right) an oscillation of the forces determined in the numerical model can be seen, which does not exist in the physically determined forces. This could be due to the absence of damping effects in the numerical model. Furthermore a gap of a few seconds in the rising branch of the forces in Figure 12 (left) can be noticed which can also be seen in Figure 10 (left) where the numerically calculated forces occur earlier than the forces determined in the physical experiments leading to comparable maximum values. The reason for this gap could not be clarified yet. It might result from a not exact initial valve opening in the physical model. However, the forces calculated with the 1D model shown in Figure 12 show a good agreement with the physical experiments, especially regarding the extrema of the forces which are the major criteria for the design process.

Figure 11: Validation case for valve discharge coefficient with 0. 8 mm/s valve opening velocity
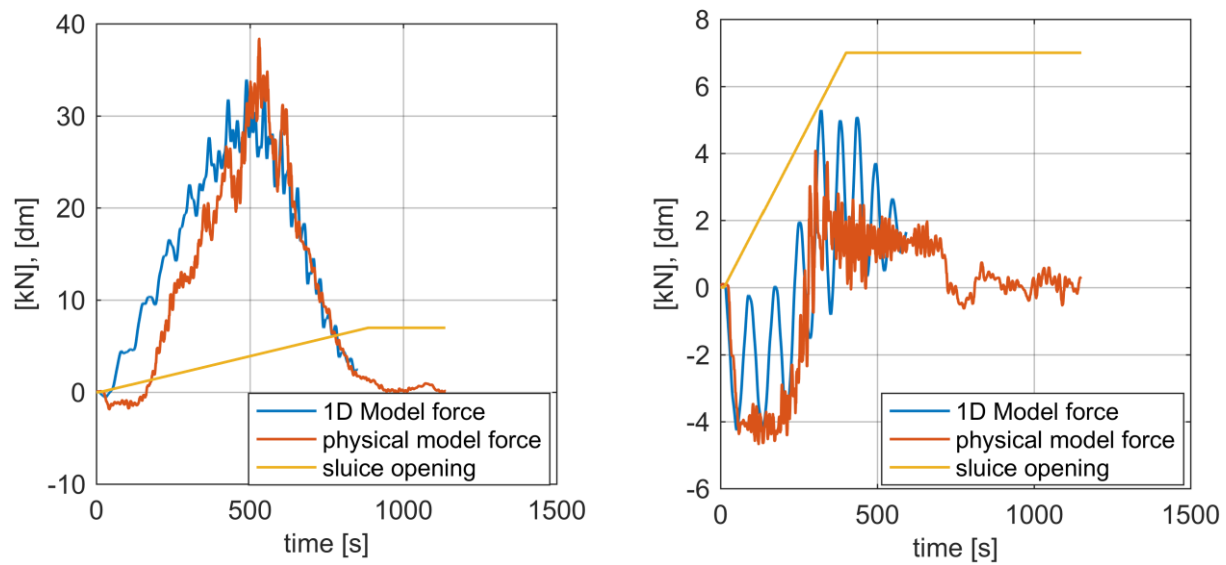
Figure 12: Validation case: Comparison of measured and simulated forces acting on a vessel for different vessel positions and valve opening velocities. left: vessel position near the upstream head, right: vessel in position in the middle of the lock chamber

4.5. Prediction of forces based only on experience

For validation the developed model was used to predict the forces acting on a ship for another lock with a different filling system, different dimensions and another vessel. Based on the experience from previous usage the calibration parameters were guessed as good as possible without regarding the results from physical investigations of this lock. Later, the predicted discharge over time and the forces acting on the vessel were compared to the results from physical experiments.

To test the accuracy of the prediction, the lock Bolzum was used. It is filled through the upstream head. To control the inflow, a segment gate instead of a sluice gate valve is used. The lock has a width of 12.5 m and a hydraulic length of 164 m. The vessel has a length of 105 m and a draught of 2.80 m. The upstream head of the lock is equipped with an energy-dissipator-grid, so that the influence of the jet is negligible. The inflow was calculated by equation (1), but the performance of the segment gate is expressed by the term $A \cdot \mu$ [m²] depending on the segment opening angle (Figure 13, left). This is done because the opening area of the segment gate is difficult to calculate due to its radial shape. Instead of the lift height a segment opening angle is prescribed over the time.

The dimensions of the lock and the ship together with the water levels at the beginning of the filling process are known values. For the performance of the segment gate the correlation between opening angle and $A \cdot \mu$ from Figure 13 (left) was taken. It was determined with a three dimensional numerical model from another project with slightly different geometry of the segment gate. With the 1D model a simulation was performed opening the segment within 800 s from 0° to 20°. The calculated discharge and the forces acting in the ship compared to the results determined from a physical model are shown in Figure 13 (right). The calculated discharge shows a good agreement with the discharge from the physical model. The maximum discharge differs about 5 %. However, the gradient of the rising discharge is slightly steeper in the physical model suggesting an underestimation of the segment gate performance in the region of small gate opening angels. Comparing the forces both lines agree qualitatively. The first flush is more distinct in the physical model, which might result from a sudden opening of the segment sealing at small opening angels. In this region the physical model is not completely applicable. Nevertheless, a good agreement between the 1D calculation and the laboratory experiments could be shown.

But note: In this case the prediction was made to a comparable lock and vessel size. Attempts to predict the forces for a sea lock which is much bigger failed. Here a basis calibration with another sea lock with comparable dimensions should be performed.

5. LIMITATIONS OF THE DEVELOPED MODEL

The 1D lock model is based on the one dimensional Saint-Venant equations. One of the fundamental estimations for applicability of these equations is a mainly one dimensional flow. Flow in the perpendicular directions is neglected in the equations. Flow in lateral direction may trigger lateral forces acting on the vessel, which cannot be determined with the 1D model. The longitudinal forces determined with the model are depending on four influencing factors:

- geometry
- valve opening velocity
- valve discharge coefficient
- jet propagation

It can be assumed that the geometry of the lock and the vessel and the valve opening velocity are known quantities and that these quantities are correctly entered in the software. The valve discharge coefficient is not known a priori and has to be determined in experiments or taken from literature, which is an uncertainty using the model. It cannot be ensured that this efficiency can be transferred to prototype size due to small adjustments in the construction which may change the hydraulic behavior of the system. Another uncertainty using the model is the parameterization of the propagation of the filling jet, which has a large influence on the forces acting on the vessel. The propagation of the jet can be determined with physical or numerical models, but this requires additional effort. The jet propagation must be parameterized by determining the force acting on a vessel as a result of the jet propagation. Thus, a scale model or on-site measurements with different vessels or vessel positions should exist to guarantee a suitable parameterization. Due to the sensitivity of the jet propagation to the size, shape and position of valve, culvert shape and gate it is difficult to predict suitable jet parameters if no information from a similar lock exists.
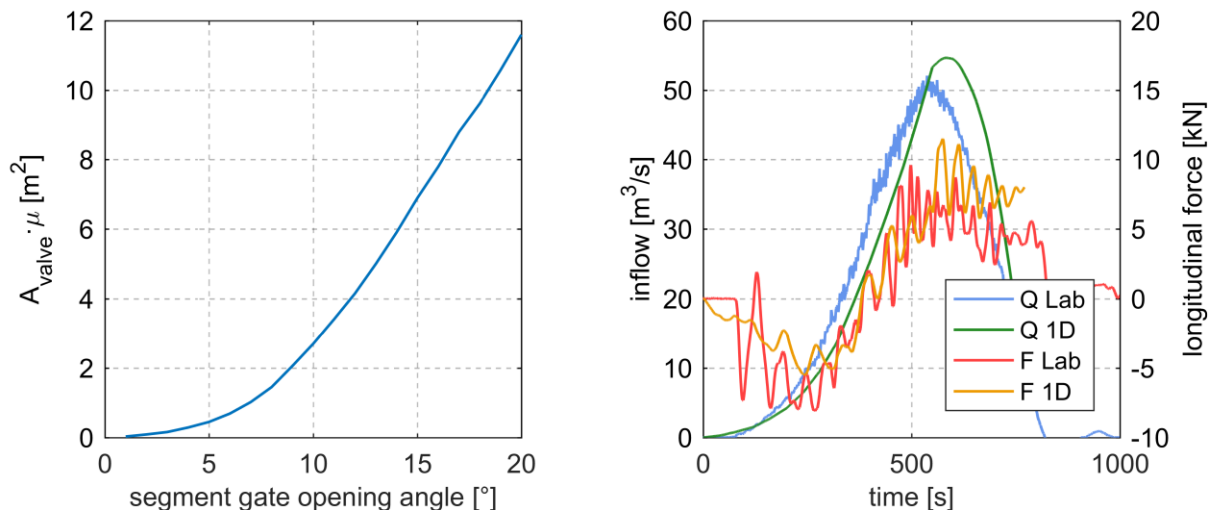
Figure 13: Left: Segment gate performance depending on the segment opening angle; right: Comparison of estimated inflow and discharge from the 1D model with the inflow and discharge determined in physical experiments

6. SUMMARY AND CONCLUSIONS

During the lock filling process forces are acting on the vessel in the lock chamber. For the design process of the filling system and to specify the valve opening velocity it is crucial to know these forces. The main hydraulic phenomena triggering forces are explained in this paper for lock filling through the head. Existing methods to determine the forces are discussed. A one dimensional model which allows the short-time prediction of the longitudinal forces is introduced and the calibration parameters and their impacts are mentioned. Due to the open data policy of the BAW, the developed software including the source code is available as open-source.

The model allows the user to calculate forces acting on a vessel during the lock filling process under different hydraulic boundary conditions in a very short time. If a physical model exists to perform a reasonable calibration a prediction of the forces occurring for different valve opening velocities or ship positions can be performed with a high certainty. This allows calculations based on data of a physical model even if the model itself does not exist anymore.

The extrapolation to locks with other geometries and filling systems is much more uncertain because the calibration parameters have to be estimated. Here the engineer has to be careful due to the effect of a bad calibration, which might underestimate the calculated forces. A working energy dissipation at the upstream head decreases the forces acting on the vessel due to a decreasing influence of the jet. Furthermore, the uncertainties due to a bad calibration of the jet propagation decrease, too.

7. NOTATION

Δh	[m]	water level difference between outer harbor and the lock chamber
μ	[-]	discharge coefficient
Q	[m³·s⁻¹]	flow rate
g	[m·s⁻²]	gravitational constant (g=9.81 m·s⁻²)
h	[m]	water level
$A_{chamber}$	[m²]	gross area in the lock chamber
A_{vessel}	[m²]	cross sectional area of the vessel
$W_{chamber}$	[m]	width of the lock chamber
m_{vessel}	[kg]	mass of the vessel
F	[N]	longitudinal force acting on the vessel
A	[m²]	overall cross sectional area
β	[-]	Boussinesq coefficient
q	[m²·s⁻¹]	specific discharge
L_{vessel}	[m]	length of the vessel
T	[s]	wave cycle time
n	[-]	time step index
A_{valve}	[m²]	valve opening area
u	[m·s⁻¹]	velocity
$L_{chamber}$	[m]	length of the lock chamber
I	[-]	slope
A_{jet}	[m²]	cross sectional area of the filling jet
Δt	[s]	time step size
Δx	[m]	distance between two cross sections
θ	[-]	Crank Nicolson factor
B_{vessel}	[m]	width of vessel
i	[-]	grid index
c_0, c_1, c_2, c_3	[-]	linear coefficient and exponent to describe jet expansion

8. REFERENCES

Belzner, F.; Merkel, J.; Gebhardt, M.; Thorenz, C. (2017): Piano Key and LabyrinthWeirs at German waterways: Recent and future research of the BAW. In Sébastien Erpicum, Frédéric Laugier, Michael Pfister, Michel Pirotton, Guy-Michel Cicero, Anton J. Schleiss (Eds.): Labyrinth and Piano Key Weirs III: CRC Press/Balkema, pp. 167–174.

Bousmar, Didier; Savary, Celine; Swartenbroekx, Catherine; Zorzon, Gil (2017): Feedback From 10 Years Of Field Measurement On Navigation Locks. In : Hydrolink Magazine, 1/2017, pp. 10–13.

Crank, J.; Nicolson, P.; Hartree, D. R. (1947): A practical method for numerical evaluation of solutions of partial differential equations of the heat-conduction type. In *Math. Proc. Camb. Phil. Soc.* 43 (01), p. 50. DOI: 10.1017/S0305004100023197.

Cunge, Jean A.; Holly, Forrest M.; Verwey, Adri (1980): Practical aspects of computational river hydraulics. Boston u.a.: Pitman (Monographs and surveys in water resources engineering, 3).

De Loor, Alexander (2016): LOCKFILL. User & Technical Manual. Deltares. Delft. Available online at http://oss.deltares.nl/documents/645319/645571/Lockfill+Manual, checked on 3/7/2018.

Free Software Foundation (2007): GNU General Public License 3. Available online at https://www.gnu.org/licenses/gpl-3.0, checked on 3/9/2018.

Gamma, Erich (2011): Design patterns. Elements of reusable object-oriented software. 39. printing. Boston: Addison-Wesley (Addison-Wesley professional computing series).

Jirka, Gerhard H.; Lang, Cornelia (2009): Einführung in die Gerinnehydraulik.

Max-Planck-Gesellschaft (2003): Berlin Declaration on Open Access to Knowledge in the Sciences and Humanities. With assistance of Prof. Dr. Martin Stratmann. Edited by Max-Planck-Gesellschaft. München. Available online at https://openaccess.mpg.de/67605/berlin_declaration_engl.pdf, updated on 2/15/2018.

Oracle (2018a): Class ResourceBundle. Edited by Oarcle. Available online at https://docs.oracle.com/javase/8/docs/api/java/util/ResourceBundle.html, checked on 3/7/2018.

Oracle (2018b): JAXB. Java Architecture for XML Binding. Edited by GitHub. Available online at https://javaee.github.io/jaxb-v2/, checked on 3/9/2018.

Partenscky, H.-W. (1986): Binnenverkehrswasserbau. Schleusenanlagen. Berlin Heidelberg NewYork Tokyo: Springer.

PIANC (2015): PIANC InCom WG 155. Ship Behaviour in Locks and Lock Approaches. With assistance of Carsten Thorenz, Jeremy R. Augustin, Didier Bousmar, Jean-Pierre Dubbelman, Arcelio Hartley, Peter Hunter et al. Edited by PIANC.

Thorenz, Carsten (2009): Computational Fluid Dynamics in lock design. State of the art. PIANC INTERNATIONAL WORKSHOP "Innovation in Navigation Lock Design". Brussels, Belgium, 2009.

Thorenz, Carsten (2010): Numerical evaluation of filling and emptying systems for the new Panama Canal locks. In : 32nd PIANC International Navigation Congress 2010. Liverpool, United Kingdom, 10 - 14 May 2010. Red Hook, NY: Curran.

Thorenz, Carsten; Anke, Jens (2013): Evaluation of ship forces for a through-the-gate filling system. Smart Rivers 2013. Liege (BE), Maastricht (NL), 2013.

Thorenz, Carsten; Belzner, Fabian; Hartung, Torsten; Schulze, Lydia (2017): Numerische Methoden zur Simulation von Schleusenfüllprozessen. In Bundesanstalt für Wasserbau (Ed.): BAW Mitteilungen 100. Kompetenz für die Wasserstraßen - Heute und in Zukunft. Forschungs- und Entwicklungsprojekte der BAW. Available online at http://henry.baw.de/bitstream/20.500.11970/102493/1/mb_100_07_Thorenz_Numerische.pdf.

Van der Ven, P.; Van Velznen, G.; O'Mahoney, T.; De Loor, A. (2015): Comparison of Scale Model Measurements and 3D CFD Simulations of Loss Coefficients and Flow Patterns for Lock Levelling Systems. In PIANC (Ed.): 7th International PIANC-SMART Rivers Conference. With assistance of Lucía Torija. Buenos Aires, Argentinia.

Vrijburcht, A. (1991): Forces on ships in a navigation lock induced by stratified flows, Stellingen.

Zhao, Bin; Zhang, Bo (2011): Comparison of different order Adams-Bashforth methods in an atmospheric general circulation model. In *Acta Meteorologica Sinica* 25 (6), pp. 754–764. DOI: 10.1007/s13351-011-0606-6.